Provided for non-commercial research and education use.
Not for reproduction, distribution or commercial use.

(This is a sample cover image for this issue. The actual cover is not yet available at this time.)

This article appeared in a journal published by Elsevier. The attached copy is furnished to the author for internal non-commercial research and education use, including for instruction at the authors institution and sharing with colleagues.

Other uses, including reproduction and distribution, or selling or licensing copies, or posting to personal, institutional or third party websites are prohibited.

In most cases authors are permitted to post their version of the article (e.g. in Word or Tex form) to their personal website or institutional repository. Authors requiring further information regarding Elsevier's archiving and manuscript policies are encouraged to visit:

http://www.elsevier.com/copyright

Author's personal copy

International Journal of Heat and Mass Transfer 55 (2012) 3349–3358

Contents lists available at SciVerse ScienceDirect

International Journal of Heat and Mass Transfer

journal homepage: www.elsevier.com/locate/ijhmt

Updated band model parameters for H_2O, CO_2, CH_4 and CO radiation at high temperature

Philippe Rivière *, Anouar Soufiani

CNRS, UPR 288, Laboratoire EM2C, Grande Voie des Vignes, F-92290 Châtenay-Malabry, France
École Centrale Paris, Grande Voie des Vignes, F-92290 Châtenay-Malabry, France

ARTICLE INFO

Article history:
Received 12 January 2012
Received in revised form 4 March 2012
Accepted 7 March 2012

Keywords:
Statistical narrow-band model
Correlated-k band model
High temperature
CO_2
H_2O
CH_4
CO infrared radiation

ABSTRACT

Statistical narrow-band (SNB) model parameters for H_2O, CO_2, CH_4 and CO, and correlated-k (CK) parameters for H_2O and CO_2 are generated from line by line calculations and recently improved spectroscopic databases in wide temperature and spectral ranges. Results from the new parameters are compared to direct line by line calculations and to results from earlier model parameters [A. Soufiani, J. Taine, High temperature gas radiative property parameters of statistical narrow-band model for H_2O, CO_2 and CO and correlated-k (ck) model for H_2O and CO_2, Int. J. Heat Mass Transfer 40 (1997) 987–991] in terms of band averaged spectral transmissivities, Planck mean absorption coefficients, and total emissivities. The comparisons show first a good agreement between updated SNB, CK and LBL results. Significant improvements on earlier parameters are observed for H_2O and CO_2, especially at very high temperatures and path lengths. Model parameters and computer programs illustrating their implementation are provided as supplementary data.

© 2012 Elsevier Ltd. All rights reserved.

1. Introduction

Accurate prediction of radiative transfer in hot gases remains a challenging issue due to the huge number of absorption lines that must be taken into account. The rigorous line by line (LBL) approach is not yet practicable for industrial or research applications involving multi-dimensional geometries and/or unsteady phenomena. Approximate models are then required to handle the spectral behavior of gas radiative properties [1–3].

Several approximate spectral models have been introduced in the last decades including global models [4–7], wide band [8,9] and narrow band models [10,11]. Principles, advantages and limitations of these models are discussed for instance in Ref. [12]. Parameters of these models have been sometimes extracted from experimental measurements [13–15] or from a combination between experimental and calculated data [16]. However, since the experiments generally do not cover the entire required ranges of wavelength, temperature and path length, the parameters are most often directly generated from spectroscopic databases (see e.g. [17] for narrow-band models).

Recently, important improvements have been achieved concerning the reliability of spectroscopic databases and their completeness for high temperature applications like combustion and atmospheric entries, and for the molecules of practical interest in these applications. The recent spectroscopic databases for H_2O and CO_2, which are the main radiating molecules among combustion products, include now transitions between very high energy levels and have been shown to be very accurate at high and medium spectral resolution.

The aim of this paper is to generate updated parameters for the correlated-k (CK) and the statistical narrow-band (SNB) models from selected recent spectroscopic data, and to compare the results from these new and from earlier parameters in terms of narrow-band transmissivities and global properties such as total emissivities and mean Planck absorption coefficients. SNB parameters are determined for H_2O, CO_2, CO and CH_4, while only H_2O and CO_2 are considered for the CK model. The paper is organized as follows. The selected spectroscopic databases are briefly introduced in Section 2 where the line by line calculations are also described. Section 3 is devoted to SNB parameter determination and to comparisons with earlier data while the developments concerning the CK model are presented in Section 4. The technical description of the parameters and computer programs, provided with this paper as supplementary data, is given in Appendix A.

2. Spectroscopic databases and line by line calculations

This section is devoted to the description of the line by line (LBL) calculations used here to provide the reference high resolution

* Corresponding author at: CNRS, UPR 288, Laboratoire EM2C, Grande Voie des Vignes, F-92290 Châtenay-Malabry, France. Tel.: +33 1 41 13 10 33; fax: +33 1 47 02 80 35.
E-mail address: philippe.riviere@em2c.ecp.fr (P. Rivière).

0017-9310/$ - see front matter © 2012 Elsevier Ltd. All rights reserved.
http://dx.doi.org/10.1016/j.ijheatmasstransfer.2012.03.019

Author's personal copy

absorption spectra from which the various model parameters have been built. For each considered molecule and thermodynamic condition, the absorption coefficient κ_ν at wavenumber ν has been calculated under the assumption of independent lines according to

$$\kappa_\nu = \sum_{\ell \to u, E_\ell < E_u} S_{\ell u}(T) n_{\text{abs}} f_{\ell u}(\nu - \nu_{\ell u}), \tag{1}$$

where the sum extends to all radiative transitions $\ell \to u$ between molecular levels ℓ and u of respective energies E_ℓ and E_u. n_{abs} designates the absorbing molecule volumetric population, $S_{\ell u}(T)$ the intensity of the transition at temperature T, $\nu_{\ell u}$ is the central wave-number of the transition, and $f_{\ell u}$ is the absorption spectral line shape. Contributing radiative transitions have been taken from recently updated spectroscopic databases (see below) which provide for each listed transition $\nu_{\ell u}$, E_ℓ, and the line intensity $S_{\ell u}(T_{\text{ref}})$ at a reference temperature T_{ref}. The intensity at any temperature T is therefore obtained according to

$$S_{\ell u}(T) = S_{\ell u}(T_{\text{ref}}) \exp\left(-\frac{E_\ell}{kT} + \frac{E_\ell}{kT_{\text{ref}}}\right) \frac{1 - e^{-\frac{hc\nu_{\ell u}}{kT}}}{1 - e^{-\frac{hc\nu_{\ell u}}{kT_{\text{ref}}}}} \frac{Q(T_{\text{ref}})}{Q(T)}, \tag{2}$$

where $Q(T)$ is the internal partition function of the molecule at temperature T, h and k designate respectively the Planck and Boltzmann constants, and c the speed of light in vacuum. It must be noticed that even if the partition function $Q(T)$ may vary greatly from one isotopologue to another, the ratio $Q(T_{\text{ref}})/Q(T)$ varies only slightly especially if only isotopologues with similar symmetry properties are considered. In the following, all ratios of partition functions will thus be evaluated from the partition function of the main isotopologue.

For all the considered molecules, a Voigt profile accounting for Doppler and collisional line broadening has been considered. Collisional broadening parameters and associated line wing cutoff $\delta\nu_{\text{cut}}$ are detailed below. A spectral discretization of 0.01 cm^{-1} has been used to calculate absorption coefficient spectra. Table 1 gives some global features of the spectroscopic databases used hereafter. Only transitions satisfying

$$n_{\text{abs}} S_{\ell u}(T) > 10^{-10}\ \text{cm}^{-2} \tag{3}$$

have been retained in Eq. (1) in order to save computational time.

2.1. CO_2 absorption spectra

The CDSD-4000 database [18] was selected since it has been shown recently to be accurate up to 4000 K at moderate spectral resolution [19]. The collisional broadening parameters are those provided in this database (air and self broadening half width at half maximum (HWHM), and the temperature dependence coefficients). A line wing cutoff $\delta\nu_{\text{cut}} = 50\ \text{cm}^{-1}$ was shown to be accurate enough. As discussed in Ref. [19], the partition function was calculated using the simple uncoupled harmonic oscillator and rigid rotor approximation, which has been shown to yield a good agreement with most recent published results up to 4000 K. Only the two main isotopologues have been accounted for, namely $^{12}C^{16}O_2$ and $^{13}C^{16}O_2$. χ correction functions of Ref. [20] have been used to account for the sub-lorentzian behavior of the collisional line shapes at temperatures below 900 K.

Table 1
Global characteristics of the spectroscopic databases used here for the main isotopologue of each species: number of transitions N_{lines}, level energy cutoff E_{cut}, maximum rotational quantum number $J_{\max}$, and line intensity cutoff S_{cut}.

Molecule	Ref.	N_{lines}	E_{cut} (cm^{-1})	$J_{\max}$	S_{cut} (cm/molecule)
CO_2	[18]	573,881,316	43,522	300	10^{-27} at 4000 K
H_2O	[21]	111,346,008	30,000	50	$\approx 10^{-27}\varepsilon(\nu,T)$[a]
CO[b]	[21]	19,119	70,000	149	2.294 10^{-166} at 296 K
CH_4	[30]	Statistical extension[c]		50	

[a] The function $\varepsilon(\nu,T)$, about 3 in the mid-IR, decreases the intensity cutoff at small wave-numbers [21].
[b] Cutoff observed in the database but not necessarily used when building it.
[c] Up to the 10th polyad around 13,500 cm^{-1}.

2.2. H_2O absorption spectra

We use for H_2O the HITEMP 2010 database [21] which was obtained by merging the well established HITRAN 2008 data [22] and a selection of lines from the extensive theoretical BT2 database [23]. The BT2 database was shown to provide accurate results by comparison with the few available experimental spectra of hot water vapor [21]. However, about ten lines in HITEMP 2010 appeared to be not reliable and have been removed in the present calculations.[1] The intensities and/or lower level energies of these lines are in strong disagreement with the original BT2 line list and some of them are too strong at high temperature and are not observed in experimental flame emission spectra (see e.g. Ref. [24]). Note however that these few lines have no significant incidence on SNB parameters and on resulting radiative transfer calculations.

The HITEMP 2010 database provides also collisional broadening parameters in the case of air- and self-broadening (HWHM) but no temperature dependence coefficient in the case of self-broadening. We have thus retained the collisional broadening parameters of Ref. [25]. In order to save computational times, a progressive line wing cutoff has been used: $\delta\nu_{\text{cut}} = 500\ \text{cm}^{-1}$ for temperatures below 2100 K, $\delta\nu_{\text{cut}} = 200\ \text{cm}^{-1}$ in the temperature range 2100–3300 K, and $\delta\nu_{\text{cut}} = 100\ \text{cm}^{-1}$ for temperatures greater than 3300 K. We used the partition function adjustments of Ref. [26]. The three main isotopologues have been accounted for in LBL calculations. At 300 K, χ correction functions of Ref. [27] have been introduced to account for non-lorentzian behavior of collisional line shapes.

2.3. CO absorption spectra

The HITEMP 2010 CO compilation [21], which is mainly based on a merge between the HITRAN data and those of Ref. [28], was retained. Air-collisional broadening parameters have been also taken from this database and a line wing cutoff $\delta\nu_{\text{cut}} = 500\ \text{cm}^{-1}$ was used. The partition function provided with the HITRAN database [22] is limited to 3000 K. At higher temperatures, we use the partition function calculated in Ref. [29]. All the six isotopologues included in HITEMP 2010 were accounted for.

2.4. CH_4 absorption spectra

We use the database provided in Ref. [30] which was obtained from a statistical extension of calculations made in the framework of an effective Hamiltonian approach. This database was shown to enable calculations of band absorptances and of total emissivities in good agreement with available experimental data up to 1500 K. Line by line calculations with this database are described in Ref. [30].

3. Statistical narrow-band model parameters

3.1. Calculation of SNB parameters

The random SNB model, based on the Mayer and Goody approach [10], is chosen here in association with the Malkmus exponential-tailed S^{-1} line intensity distribution [31] to express

[1] The positions of these lines are 903.53279, 914.60674, 933.51275, 2267.12826, 2520.43998, 2541.10800, 7404.93633, 7495.4980, 8547.6857, and 10526.27491 cm^{-1}.

Author's personal copy

column transmissivities. Although other line intensity distributions may be preferred in the Doppler broadening regime for low pressure applications [32], the exponential-tailed S^{-1} distribution was found to be the most accurate for Lorentz line profiles prevailing at atmospheric or higher pressures [12]. The mean transmissivity of a uniform column of length ℓ, at total pressure p, and with a molar fraction x of the absorbing species, averaged on a narrow-band of width $\Delta\nu$ is given by

$$\bar{\tau} = \exp\left[-\frac{2\bar{\gamma}}{\bar{\delta}}\left(\sqrt{1+\frac{xp\ell\bar{k}\bar{\delta}}{\bar{\gamma}}}-1\right)\right]. \tag{4}$$

The parameters $\bar{k}$, $\bar{\gamma}$ and $\bar{\delta}$ have their usual meaning, i.e., the mean line intensity to line spacing ratio, the average line Lorentz half-width, and the mean line spacing, as identified in the strong absorption limit. The parameters $\bar{k}$ and $\bar{\delta}$ are extracted from line by line calculations where each absorbing species was diluted in air, except for H_2O which was diluted in N_2 with a molar fraction $x_{H2O} = 0.1$. In practice, the parameter $\bar{k}$ was calculated as the mean absorption coefficient per unit partial pressure of the absorbing species

$$\bar{k} = \frac{1}{xp}\int_{\Delta\nu}\kappa_\nu d\nu. \tag{5}$$

This relation results from the identification of the average transmissivity in the weak absorption limit $xp\ell\bar{k}\bar{\delta}/\bar{\gamma} << 1$. The parameter $\bar{k}$ remains practically insensitive to mixture composition and to the total pressure as far as line widths remain small in comparison with $\Delta\nu$. It only depends on the temperature and on the considered narrow band. The parameter $\bar{\delta}$ was then determined from a least-square adjustment between model predictions and line by line calculations of column averaged transmissivities for various values of the column length ℓ (curves of growth). The set of ℓ values was chosen such that the theoretical transmissivities cover the range 0.02–0.95 including 20 regularly spaced values. For this adjustment, SNB transmissivities were calculated from Eq. (4) using the average Lorentz line-widths

$$\bar{\gamma}_{H_2O} = \frac{p}{p_s}\left\{0.462\frac{T_s}{T}x_{H_2O} + \left(\frac{T_s}{T}\right)^{0.5}\times[0.0792(1-x_{CO_2}-x_{O_2}) + 0.106x_{CO_2} + 0.036x_{O_2}]\right\}, \tag{6}$$

$$\bar{\gamma}_{CO_2} = \frac{p}{p_s}\left(\frac{T_s}{T}\right)^{0.7}\left[0.07x_{CO_2} + 0.058(1-x_{CO_2}-x_{H_2O}) + 0.1x_{H_2O}\right], \tag{7}$$

$$\bar{\gamma}_{CO} = \frac{p}{p_s}\left\{0.075x_{CO_2}\left(\frac{T_s}{T}\right)^{0.6} + 0.06(1-x_{CO_2}-x_{H_2O})\left(\frac{T_s}{T}\right)^{0.7} + 0.12x_{H_2O}\left(\frac{T_s}{T}\right)^{0.82}\right\}, \tag{8}$$

$$\bar{\gamma}_{CH_4} = 0.051\frac{p}{p_s}\left(\frac{T_s}{T}\right)^{0.75}, \tag{9}$$

where $p_s = 1$ atm, $T_s = 296$ K, and $\bar{\gamma}$ is expressed in cm^{-1}. It is important to note here that Eq. 4 must be used with these mean line widths in order to be consistent with the adjusted parameter $\bar{\delta}$. On the other hand, although Eq. 4 only strictly holds for Lorentz line shapes, the line-by-line calculations used for the adjustment of $\bar{\delta}$ were carried out using Voigt line profiles in order to provide better accuracy at very high temperatures.

SNB parameters have been calculated from the spectroscopic databases described in Section 2 with 25 cm^{-1} spectral resolution.

Table 2
Minimum and maximum SNB band centers and total number of bands.

Molecule	ν_{min} (cm^{-1})	ν_{max} (cm^{-1})	Number of bands
H_2O	50	11,250	449
CO_2	250	8300	323
CO	1600	6425	194
CH_4	25	6200	248

The temperature range 300–5000 K was considered for H_2O, CO_2 and CO, while it was limited to 300–2000 K for CH_4 due to the decomposition of this molecule at higher temperatures. The covered spectral ranges are given in Table 2. No transparency regions were included inside these ranges.

3.2. SNB results and comparisons with earlier data

3.2.1. Averaged transmission spectra

Figs. 1–4 show comparisons between column transmissivities, averaged over 25 cm^{-1}, obtained from LBL and SNB calculations for H_2O, CO_2, CO and CH_4, respectively, in selected important spectral ranges. LBL results were averaged over 25 cm^{-1} to allow comparisons with SNB results. The maximum temperature considered in these figures for H_2O, CO_2 and CO is 2900 K and corresponds to the limit of the earlier SNB parameters [17]. The results from these earlier parameters are also shown on Figs. 1–3.

The comparison between LBL and new SNB results shows an excellent agreement illustrating the quality of model parameter adjustments. This is particularly true at high temperatures since the density of effective lines increases with the temperature. Small discrepancies appear for the diatomic molecule CO in the fundamental vibrational region (left graphs in Fig. 3). Line density is indeed smaller for CO and the lines are quite regularly spaced. Then, LBL curves of growth cannot be exactly represented by random SNB curves of growth. The differences remain however limited to a few percents.

The comparison between earlier and new SNB results shows that the differences increase with the temperature. This behavior simply reflects the differences between earlier and new spectroscopic data, and the differences in internal partition functions. While the agreement is very satisfactory for H_2O and CO_2 at 1500 K, a significant scatter is observed at 2900 K. Fig. 2 shows clearly that transitions characterized by very high energy levels (in the spectral region 1900–2150 cm^{-1}) are missing in the earlier EM2C spectroscopic database [33]. A thorough analysis and comparison between this database and CDSD4000 are given in Refs. [34,19]. The small discrepancies observed for CO are mostly due to the differences between earlier (harmonic oscillator and rigid rotor) and new (based on direct summation on energy levels) internal partition functions.

3.2.2. Planck mean absorption coefficient and total emissivities

For practical heat transfer considerations, it is also interesting to compare total radiative properties obtained from the recent selected spectroscopic databases and LBL calculations, from the new, and from the earlier SNB parameters. The Planck mean absorption coefficient was calculated according to

$$K_{LBL,P}(T) = \frac{\pi}{\sigma T^4}\int_0^\infty \frac{\kappa_\nu(T)}{xp} I^0_\nu(T)d\nu, \tag{10}$$

using LBL calculations, and according to

$$K_{SNB,P}(T) = \frac{\pi}{\sigma T^4}\sum_{\text{bands}\ b}\bar{k}_b(T)I^0_{\nu_b}(T)\Delta\nu, \tag{11}$$

for SNB models, where σ is the Stefan–Boltzmann constant and $I^0_\nu(T)$ the spectral equilibrium intensity at temperature T. Fig. 5 shows the

Author's personal copy

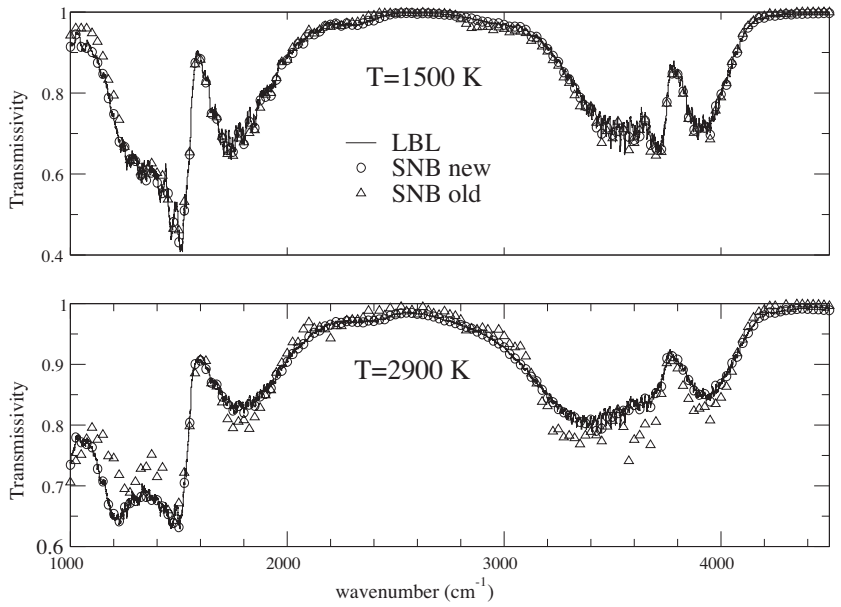

Fig. 1. H_2O transmissivity in the 1000–4500 cm^{-1} spectral range at 1500 K and 2900 K. $x_{H_2O} = 0.1$, $\ell = 100$ cm, $p = 1$ atm.

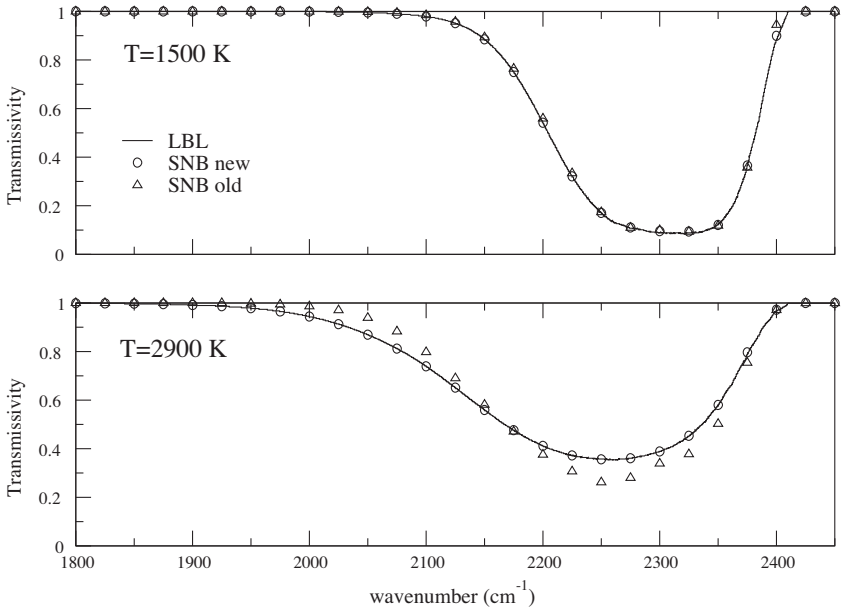

Fig. 2. CO_2 transmissivity in the 4.3 μm region at 1500 K and 2900 K. $x_{CO_2} = 0.1$, $\ell = 10$ cm, $p = 1$ atm.

computed Planck mean absorption coefficients for the four molecules and the differences between earlier SNB values and new LBL calculations for H_2O, CO_2 and CO. The differences between new LBL and new SNB calculations (not shown on the lower part of the figure) remain smaller than 0.2% for the whole considered temperature range. These very small differences result from the use of a constant equilibrium intensity $I^0_{\nu_b}$ inside each band in association with the SNB model instead of a continuous one for LBL calculations.

The most important difference between earlier SNB and new Planck mean absorption coefficients occurs for H_2O at low temperatures and reaches 12% at 300 K. This difference is due to the wavenumber cutoff at 150 cm^{-1} in the earlier SNB parameters. A significant part of the rotational band was not accounted for. Except for H_2O at low temperature, the differences between earlier and updated data remain limited to ±7% up to 2900 K. This means that the higher discrepancies observed locally on Figs. 1 and 2 offset each other between different spectral ranges.

Earlier and new data were also compared in terms of total emissivities computed following

$$\epsilon_{tot}(x,p,\ell,T) = \frac{\pi}{\sigma T^4}\int_0^\infty (1 - exp(-\kappa_\nu(x,p,T)\ell))I^0_\nu(T)d\nu, \tag{12}$$

from LBL calculations, and following

$$\epsilon_{tot}(x,p,\ell,T) = \frac{\pi}{\sigma T^4}\sum_{\text{bands } b}(1-\bar{\tau}_b(x,p,\ell,T))I^0_{\nu_b}(T)\Delta\nu, \tag{13}$$

for SNB models. The results are shown on Figs. 6–9 for H_2O, CO_2, CO and CH_4, respectively, and for various optical path lengths. Here also, a very good agreement between LBL calculations and new SNB results is generally obtained. Relative differences up to 13%

Author's personal copy

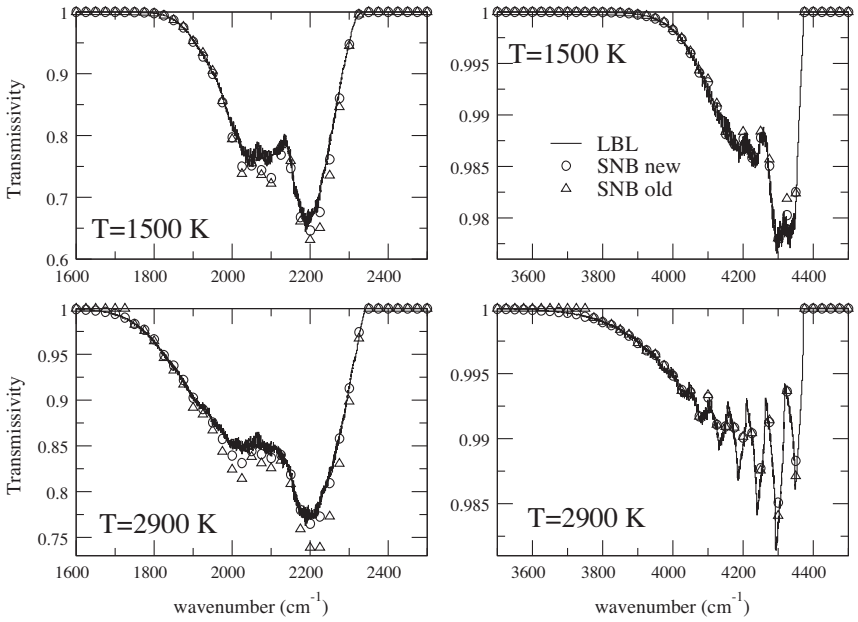

Fig. 3. CO transmissivity in the fundamental and overtone vibrational regions at 1500 K and 2900 K. $x_{CO} = 0.01$, $\ell = 1000$ cm, $p = 1$ atm.

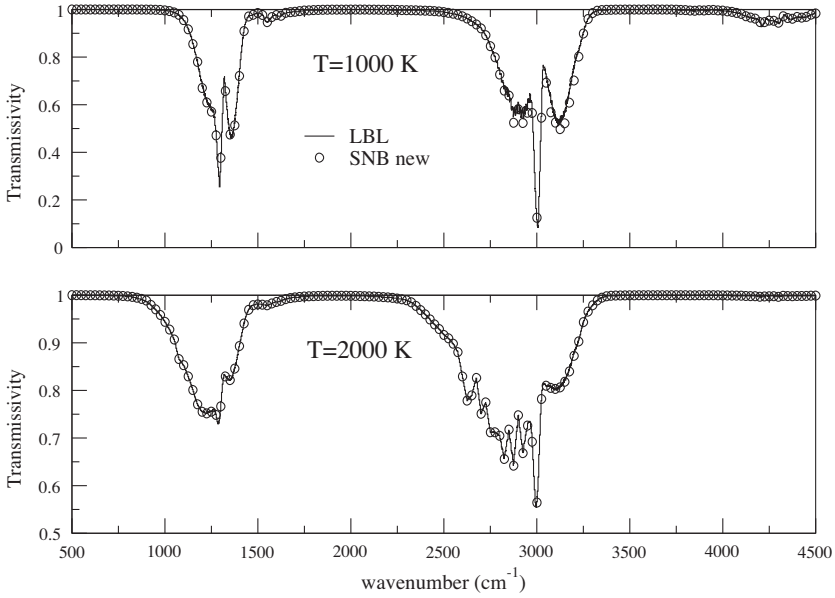

Fig. 4. CH_4 transmissivity at 1000 K and 2000 K. $x_{CH_4} = 0.01$, $\ell = 500$ cm, $p = 1$ atm.

are however observed for CO at intermediate optical thicknesses and moderate temperatures. These differences are due, as explained above, to the less easy adjustments of the curves of growth for this diatomic molecule.

Concerning H_2O, significant discrepancies between earlier and new SNB results are again observed at room temperature, due to the wider spectral range considered for the new parameters. Fig. 6 shows also that, at high temperature and for very important optical path lengths, earlier SNB parameters underestimate the total emissivity while they slightly overestimate it for small path lengths. The counterbalance between different spectral regions discussed above becomes less effective for total emissivities of optically thick columns since emission tends to be saturated in the central regions of the vibrational bands and can no more increase with the path length. This effect is much more pronounced for CO_2 as shown in Fig. 7. It is clearly due to the different spread of vibrational bands at high temperature (see Fig. 2), which results from missing high energy level lines in the earlier spectroscopic database and from the different partition functions [19]. However, for applications below typically 2500 K and path lengths smaller than typically 20 cm atm of pure CO_2, the underestimation remains limited to about 20%. For CO, earlier and new SNB results are generally in good agreement highlighting the accuracy of the earlier spectroscopic data. Significant differences (reaching 30%) are observed for the highest path lengths and the lowest temperatures. This is simply due to the wider spectral range considered in the new calculations.

3.2.3. Gas mixture composition effects on SNB accuracy

The results presented above were related to pure absorbing species diluted in air or in N_2. It is interesting to check the validity of

Author's personal copy

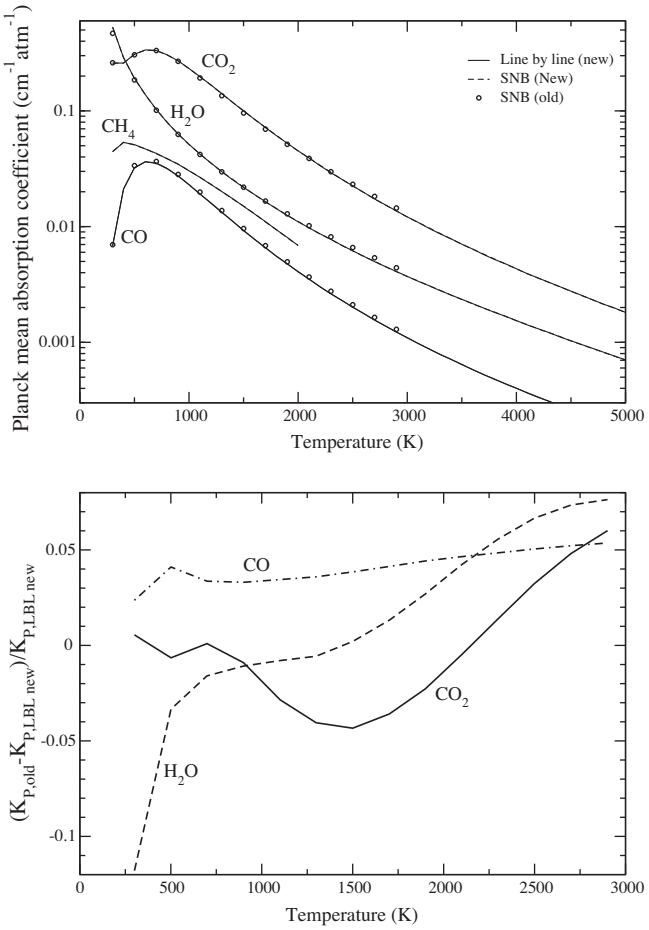

Fig. 5. Upper part: Planck mean absorption coefficients obtained from LBL calculations and the recent spectroscopic databases, from the new and from the earlier SNB parameters. Results from the new SNB parameters are indistinguishable from LBL calculations. Lower part: relative differences between earlier SNB results and the results from new LBL calculations.

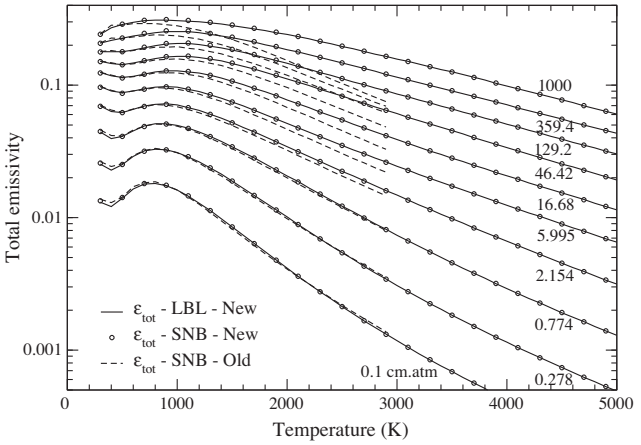

Fig. 7. Total emissivity of CO_2 diluted in N_2. $x_{CO_2} = 0.1$, $p = 1$ atm, the $xp\ell$ product varies logarithmically between 0.1 and 1000 cm atm.

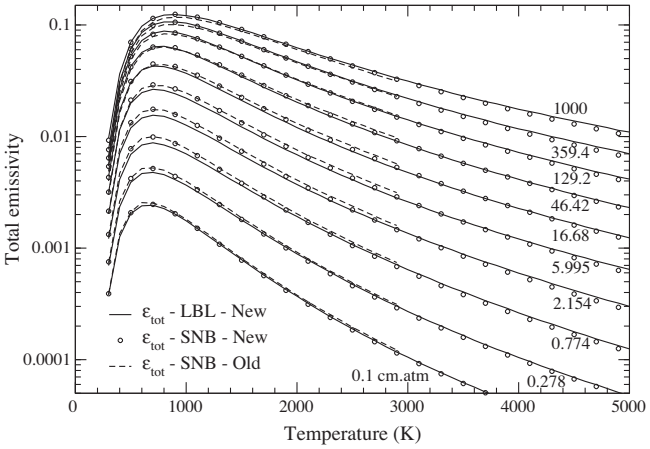

Fig. 8. Total emissivity of CO diluted in N_2. $x_{CO} = 0.01$, $p = 1$ atm, the $xp\ell$ product varies logarithmically between 0.1 and 1000 cm atm.

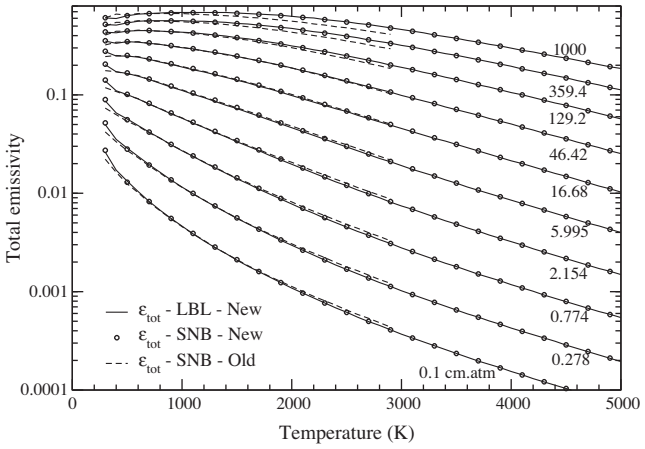

Fig. 6. Total emissivity of H_2O diluted in N_2. $x_{H_2O} = 0.1$, $p = 1$ atm, the $xp\ell$ product varies logarithmically between 0.1 and 1000 cm atm.

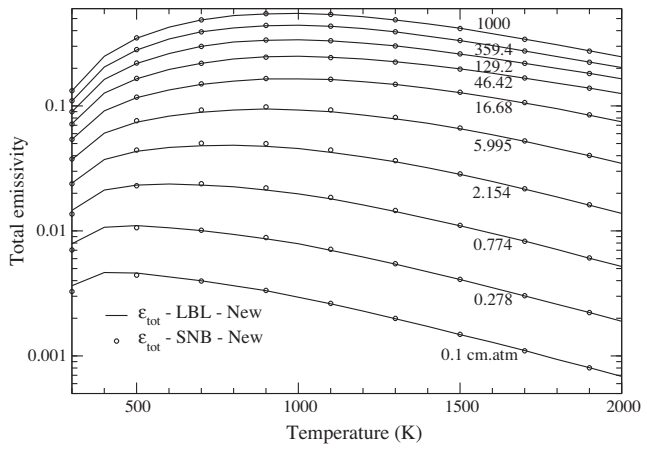

Fig. 9. Total emissivity of CH_4 diluted in N_2. $x_{CH_4} = 0.01$, $p = 1$ atm, the $xp\ell$ product varies logarithmically between 0.1 and 1000 cm atm.

the SNB model in the case of mixtures of absorbing species with variable composition and molar fractions.

The first phenomenon which may induce some inaccuracies is the variation of line broadening parameters with mixture composition. This question arises especially for H_2O due to the important resonant self-broadening compared to foreign broadening (see Eqs. (6)–(9)), particularly at low-temperature. We compare in Fig. 10 the transmissivities of different H_2O–N_2 mixture columns characterized by the same path length $x_{H2O}p\ell$ but with different H_2O molar fractions at 1500 K and 1 atm. The column transmissivities

Author's personal copy

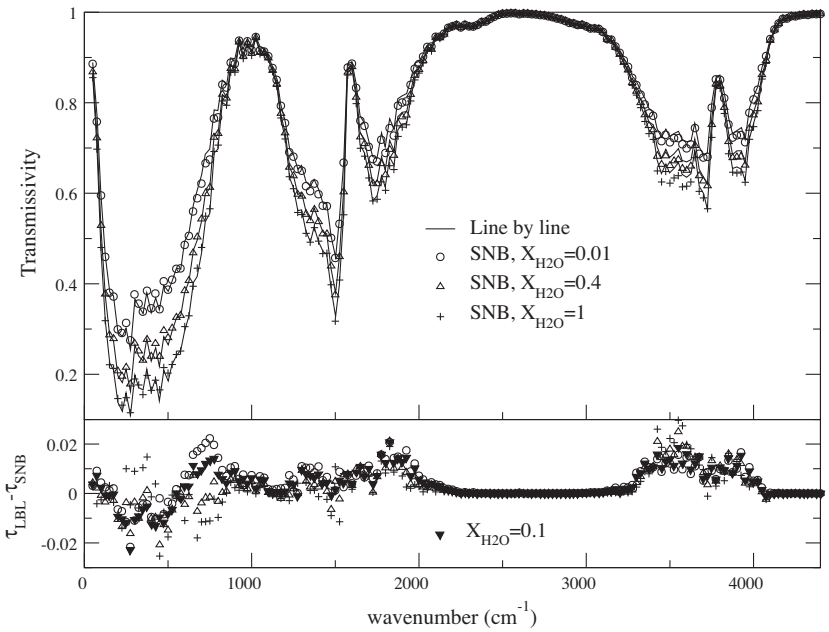

Fig. 10. Effects of H_2O line self-broadening on the accuracy of the statistical model. The upper part of the figure shows the transmissivity averaged over 25 cm^{-1} of H_2O–N_2 mixtures characterized by the same product $x_{H2O}p\ell$ = 10 cm atm at 1500 K and 1 atm but with variable H_2O molar fraction. The lower part shows differences between LBL and SNB results for x_{H_2O} = 0.01, 0.4, and 1, and for x_{H_2O} = 0.1 which is the molar fraction used to adjust SNB parameters.

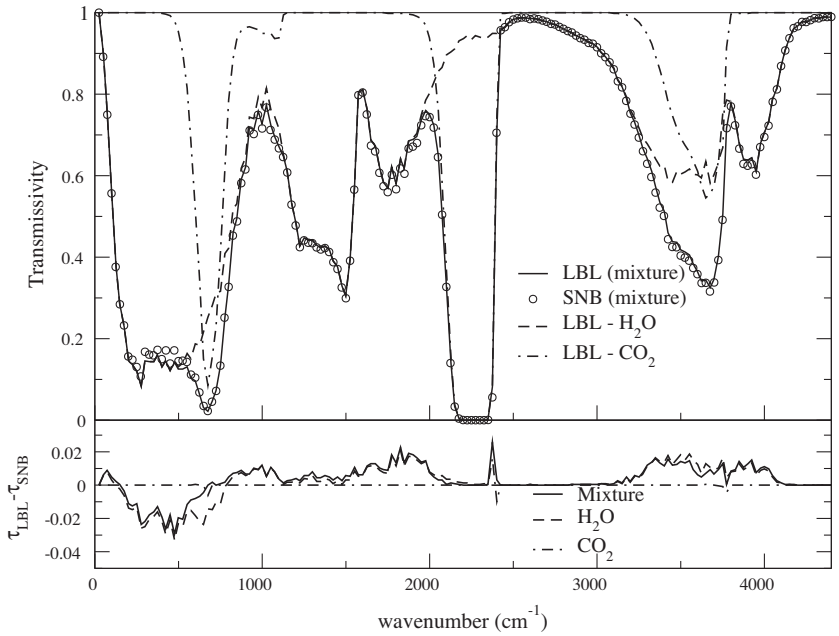

Fig. 11. Transmissivity of a H_2O–CO_2–N_2 mixture with x_{H_2O} = 0.2 and x_{CO_2} = 0.1 at T = 2000 K, p = 1 atm and ℓ = 100 cm. The lower part of the figure shows the differences between LBL and SNB results for H_2O and CO_2 alone and for the gas mixture.

are shown to decrease when increasing x_{H2O} due to self-broadening which increases line widths. The lower part of Fig. 10 shows that this behavior is well captured by the SNB model. Indeed, changing x_{H2O} does not significantly downgrade the accuracy of SNB calculations when used with the scaling of the average collisional half-width given by Eq. (6).

The second issue concerns the transmissivity of two or more species in overlapping spectral regions. This is typically the case in combustion applications involving H_2O and CO_2 in the 2.7 μm region. The average transmissivity of a mixture of absorbing species may generally be approximated as the product of individual transmissivities. This approximation results from the uncorrelation of the absorption spectra of the different species, and was already discussed and validated in earlier studies (see e.g. Ref. [12]). However, using new spectroscopic data bases, it is important to check again the validity of this multiplication property. Fig. 11 shows the transmissivity of a H_2O–CO_2–N_2 mixture with a composition representative of methane-air combustion products leading to comparable contributions of H_2O and CO_2 near 2.7 μm. The column length (100 cm) is chosen such that the medium is neither in the weak nor in the strong absorption limit in this spectral region. The differences between LBL and SNB results, shown in the lower

Author's personal copy

Table 3
Quadrature points and weights for the CK model.

j	g_j	ω_j
1	0.	0.045
2	0.155405848	0.245
3	0.45	0.32
4	0.74459415	0.245
5	0.9	0.056111111
6	0.935505103	0.051248583
7	0.984494897	0.037640306

part of the figure, indicate that the use of transmissivity products does not introduce higher errors in comparison with the differences observed for pure species.

4. Correlated-k model parameters

Correlated-k parameters have been calculated for H_2O and CO_2 from HITEMP 2010 and CDSD-4000 spectroscopic databases, respectively, at atmospheric pressure. In the framework of this model, the intensity $\bar{I}_b$ averaged over a spectral band $\Delta\nu_b$ is obtained by replacing the frequency integration by a quadrature applied to the reordered absorption spectrum

$$\bar{I}_b = \sum_{j=1}^{Nq} \omega_j I_{g_j}, \tag{14}$$

where g_j and ω_j are respectively the abscissae and the weights of the quadrature, and where the partial intensity I_{g_j} satisfies the radiative transfer equation (without scattering)

$$\boldsymbol{u} \cdot \nabla I_{g_j} = k_{g_j}\left(I^0_{\nu_b} - I_{g_j}\right). \tag{15}$$

In this equation, $\mathbf{u}$ is the propagation direction and k_{g_j} is the reordered absorption coefficient at quadrature abscissa g_j. In practise, we use the same seven point quadrature as in Ref. [17], which is given for the sake of completeness in Table 3. The parameters k_{g_j} have been directly obtained by reordering the high resolution absorption coefficient spectra and taking their values at the points g_j of the band $\Delta\nu_b$, scaled to the range [0,1].

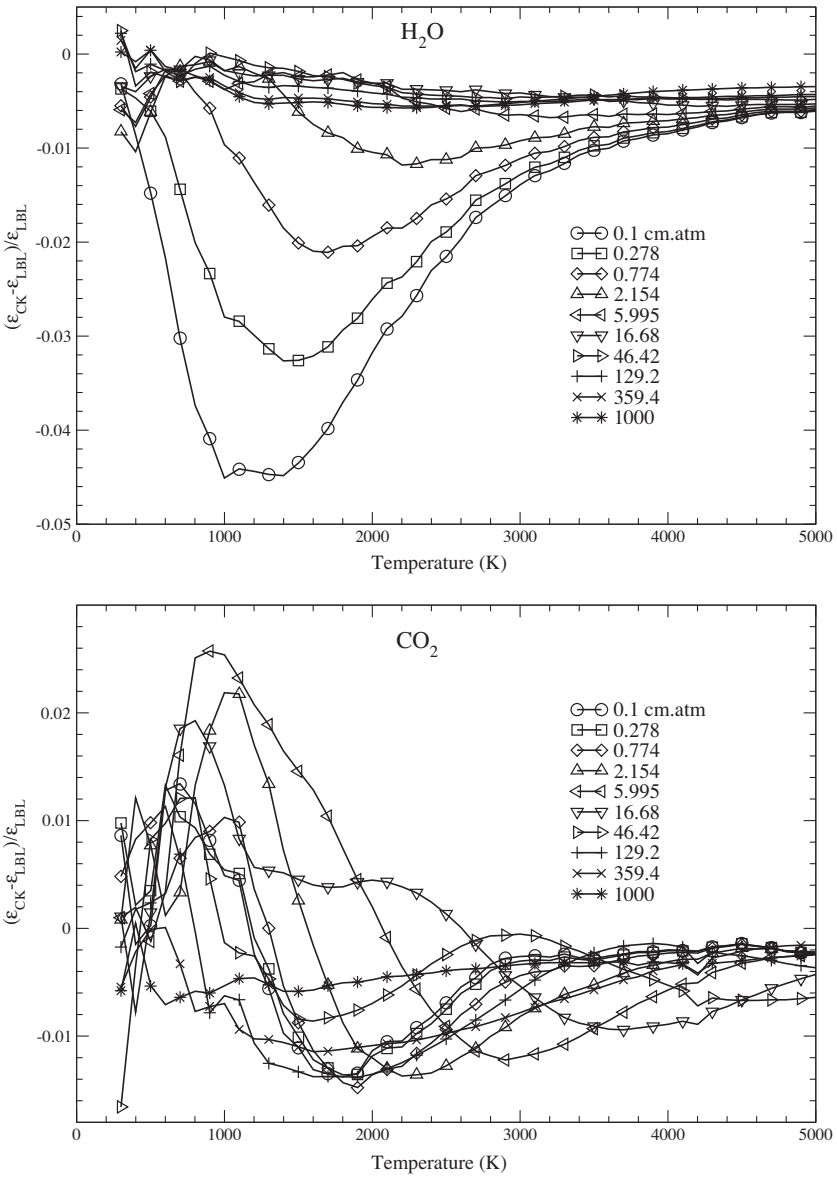

Fig. 12. Relative differences between total emissivities computed from the CK model and from LBL calculations. Upper part: H_2O with $x_{H_2O} = 0.01$. Lower part: CO_2 with $x_{CO_2} = 0.1$. The path length varies logarithmically between 0.1 and 1000 cm atm for both molecules.

Author's personal copy

Table 4
Optimized spectral discretization for the CK model.

Band centers (cm^{-1})	Number of bands	Band width (cm^{-1})	Species
62.5–212.5	4	50	H_2O
262.5–362.5	3	50	H_2O, CO_2
437.5–1137.5	8	100	H_2O, CO_2
1262.5–2162.5	7	150	H_2O, CO_2
2325.0	1	175	H_2O, CO_2
2512.5–4112.5	9	200	H_2O, CO_2
4362.5–6162.5	7	300	H_2O, CO_2
6512.5–8112.5	5	400	H_2O, CO_2
8512.5–10112.5	5	400	H_2O
10537.5	1	450	H_2O
11012.5	1	500	H_2O

In order to reduce the computational cost when using the CK model, band widths have been optimized to yield almost constant relative variations of the Planck function inside each band. Band widths for H_2O and CO_2 are given in Appendix A.

CO_2 CK parameters have been only tabulated versus temperature, since CO_2 collisional line widths depend weakly on mixture composition. In the case of H_2O, the parameters have also been tabulated versus H_2O molar fractions as detailed in Appendix A.

The global accuracy of CK parameters has been checked by comparing the total emissivities calculated according to

$$\epsilon_{tot}(x,p,\ell,T)=\frac{\pi}{\sigma T^4}\sum_{\text{bands } b}\left\{1-\sum_j \omega_j \exp[-k_{g_j}(x,p,T)\ell]\right\}I^0_{\nu_b}(T)\Delta\nu_b, \tag{16}$$

with LBL total emissivities. The relative differences between CK and LBL calculations, shown in Fig. 12, are limited to a few percents for both H_2O and CO_2. The highest differences are observed for H_2O and the smallest path lengths, for which the optimized quadrature is not sufficiently refined for high g values.

CK parameters were not calculated here for CH_4 and CO since the use of this model for mixtures containing many absorbing species with overlapping spectra becomes computationally expensive. However, if molar fraction ratios may be considered as spatially uniform for such mixtures, dedicated CK parameters can be easily generated from SNB parameters (see e.g. [35]) considering the mixture as a single absorbing species.

5. Conclusion

The recent improvement of spectroscopic databases has enabled the development in this study of more accurate parameters of the SNB model for H_2O, CO_2, CO and CH_4, and of the CK model for H_2O and CO_2. These parameters are suitable for radiative transfer calculations in high temperatures applications like combustion, atmospheric entries or nuclear reactor safety. They cover wider temperature and spectral ranges in comparison with previous data. A detailed comparison between earlier [17] and new parameter results has been carried out in terms of narrow-band transmissivities, Planck mean absorption coefficients and total emissivities. It is shown that the old set of model parameters was roughly sufficient for temperatures below typically 2500 K and for moderate path lengths. The higher differences are observed for CO_2 at very high temperatures and optical paths. The total emissivity calculated with the old set of parameters underestimates the new calculations by about 25% at 2500 K and 100 cm atm of pure CO_2 for instance. The new set of parameters allows accurate radiative transfer calculations at higher temperatures for which very hot lines were missing or inaccurately predicted in earlier spectroscopic databases. The extension of the spectral range also led to significant improvements for H_2O and CO at low temperatures and strong optical thicknesses. SNB parameters were tabulated with a 25 cm^{-1} spectral resolution but this resolution can be easily downgraded to reduce the number of solutions of the radiative transfer equation. In the same manner, SNB parameters may serve as a reference to build global model parameters or CK parameters in different pressure and composition conditions.

Acknowledgments

Computational facilities were made available by the Institut de Développement et des Ressources Informatiques Scientifiques (IDRIS), the CNRS Computer Center in Orsay, France.

Appendix A. Description of the supplementary data

We summarize in this appendix the main features and the organization of SNB and CK data, and of some computer codes provided to illustrate their implementation. These programs are self commented and show how to read and use the parameters.

A.1. SNB parameters and Fortran program

For the four considered molecules, SNB parameters have been generated considering 25 cm^{-1} band widths. The minimum and maximum band centers are given in Table 2. The covered temperature range is 300–5000 K for H_2O, CO_2 and CO, and 300–2000 K for CH_4, with a temperature step equal to 100 K. For each molecule, SNB parameters are gathered in a single file (SNBH2O, SNBCO2, SNBCO, SNBCH4) which contains successively the parameters $\bar{k}$ in $cm^{-1}.atm^{-1}$, and $1/\bar{\delta}$ in cm.

The computer code snbnew.f90 (written in Fortran90) enables the calculation of the spectral transmissivity, and of the spectral intensity, averaged over 25 cm^{-1}, at the exit of a non-uniform column containing a mixture of $H_2O/CO_2/CO/CH_4$/transparent gas mixture. The transparent gas is assumed to be N_2. The classical Curtis–Godson approximation is used [12] and the transmissivity of the gaseous mixture is assumed to be equal to the product of single species transmissivities, which constitutes an excellent approximation. The gaseous column may also contain non-scattering soot particles whose absorption coefficient is assumed equal to $\kappa_{\nu,soot} = 5.5\, f_v \nu$, where f_v is soot volume fraction, ν the wavenumber, and where $\kappa_{\nu,soot}$ and ν have the same units.

A.2. CK parameters and programs

The CK parameters have been generated for H_2O and CO_2 at atmospheric pressure. The seven-point quadrature given in Table 3 is used to calculate the absorption coefficients k_{g_j} at quadrature points g_j. In order to get more accurate temperature interpolations, the stored parameters are

$$k^*_{g_j}=\frac{k_{g_j}TQ_a(T)}{x_a}, \tag{A.1}$$

instead of k_{g_j}, where $Q_a(T)$ and x_a are the partition function and the molar fraction of the absorbing species a. The partition functions $Q_{H_2O}(T)$ and $Q_{CO_2}(T)$ are given in the programs ck_h2o_51.f90 and ck_co2_40.f90 which are provided to illustrate the calculation of uniform column transmissivities for H_2O and CO_2, respectively, with the CK model. As the CK model requires 7 solutions of the radiative transfer equation for each spectral band, band widths have been optimized according to the following criteria: (i) band widths are not uniform as for the SNB model; they are chosen so that the relative variations of the Planck's function inside each band are similar, (ii) the bands must cover the 25 cm^{-1} wide SNB bands in order to allow spectral comparisons, (iii) the same bands must be chosen

Author's personal copy

for H_2O and CO_2 in the overlapping spectral regions. The resulting spectral discretization, given in Table 4, contains 51 bands for H_2O and 40 bands for CO_2.

The parameters $k^*_{g_j}$ (in $cm^{-1}.K$) have been stored, as for the SNB model, from 300 to 5000 K with a 100 K temperature step. For H_2O, they have also been tabulated for 5 values of x_{H_2O}, namely 0.01, 0.1, 0.4, 0.66 and 1. A simple linear interpolation is sufficient for any other molar fraction. For CO_2, the parameters $k^*_{g_j}$ have been deduced from LBL calculations with $x_{CO_2} = 0.1$. The parameters are stored in a single file for each molecule (CKH_2O and $CKCO_2$).

References

[1] R. Johansson, K. Andersson, B. Leckner, H. Thunman, Models for gaseous radiative heat transfer applied to oxy-fuel conditions in boilers, Int. J. Heat Mass Transfer 53 (1-3) (2010) 220–230.

[2] H. Chu, F. Liu, H. Zhou, Calculations of gas thermal radiation transfer in one-dimensional planar enclosure using lbl and snb models, Int. J. Heat Mass Transfer 54 (21-22) (2011) 4736–4745.

[3] R.G. dos Santos, M. Lecanu, S. Ducruix, O. Gicquel, E. Iacona, D. Veynante, Coupled large eddy simulations of turbulent combustion and radiative heat transfer, Combust. Flame 152 (3) (2008) 387–400.

[4] H. Hottel, A. Sarofim, Radiative Transfer, McGraw-Hill, 1967.

[5] M. Denison, B. Webb, A spectral-line-based weighted-sum-of-gray-gases model for arbitrary RTE solvers, J. Heat Transfer 115 (1993) 1004–1012.

[6] L. Pierrot, P. Rivière, A. Soufiani, J. Taine, A fictitious-gas-based absorption distribution function global model for radiative transfer in hot gases, J. Quant. Spectrosc. Radiat. Transfer 62 (5) (1999) 609–624.

[7] M.F. Modest, H. Zhang, The full-spectrum correlated-k distribution for thermal radiation from molecular gas-particulate mixtures, J. Heat Transfer 124 (1) (2002) 30–38.

[8] D. Edwards, Molecular gas band radiation, Adv. Heat Transfer 12 (1976) 115–193.

[9] J. He, W.L. Cheng, R.O. Buckius, Wide band cumulative absorption coefficient distribution model for overlapping absorption in H_2O and CO_2 mixtures, Int. J. Heat Mass Transfer 51 (5-6) (2008) 1115–1129.

[10] R. Goody, Y. Yung, Atmospheric radiation, 2nd ed., Oxford, 1989.

[11] A. Lacis, V. Oinas, A description of the correlated-k distribution method for modeling nongray gaseous absorption thermal emission and multiple scattering in vertically inhomogeneous atmospheres, J. Geophys. Res. 96 (1991) 9027–9063.

[12] J. Taine, A. Soufiani, Gas ir radiative properties: from spectroscopic data to approximate models, Adv. Heat Transfer 33 (1999) 295–414.

[13] C. Ludwig, W. Malkmus, J. Reardon, J. Thomson, Handbook of infrared radiation from combustion gases, Technical Report NASA SP-3080, Marshall Space Flight Center, National Aeronautics and Space Administration, Washington, D.C. 1973.

[14] W. Grosshandler, RADCAL: A narrow-band model for radiation calculations in a combustion environment, Technical Report Technical Note 1402, NIST, 1993.

[15] W. Phillips, Band-model parameters for 4.3 μm CO2 band in the 300–1000 K temperature region, J. Quant. Spectrosc. Radiat. Transfer 48 (1) (1992) 91–104.

[16] B. Leckner, Spectral and total emissivity of water vapor and carbon dioxide, Combust. Flame 19 (1972) 33–48.

[17] A. Soufiani, J. Taine, High temperature gas radiative property parameters of statistical narrow-band model for H_2O, CO_2 and CO and correlated-k (ck) model for H_2O and CO_2, Int. J. Heat Mass Transfer 40 (1997) 987–991.

[18] S.A. Tashkun, V.I. Perevalov, L.H. Coudert, Cdsd-4000: High-resolution, high-temperature carbon dioxide spectroscopic databank, J. Quant. Spectrosc. Radiat. Transfer 112 (9) (2011) 1403–1410.

[19] S. Depraz, M.-Y. Perrin, P. Rivière, A. Soufiani, Infrared emission spectroscopy of CO_2 at high temperature. Part II: Experimental results and comparisons with spectroscopic databases, J. Quant. Spectrosc. Radiat. Transfer 113 (2012) 14–25.

[20] M.-Y. Perrin, J.-M. Hartmann, Temperature-dependent measurements and modeling of absorption by CO_2–N_2 mixtures in the far line-wings of the 4.3 μm CO_2 band, J. Quant. Spectrosc. Radiat. Transfer 42 (4) (1989) 311–317.

[21] L.S. Rothman, I.E. Gordon, R.J. Barber, H. Dothe, R.R. Gamache, A. Goldman, V.I. Perevalov, S.A. Tashkun, J. Tennyson, Hitemp, the high-temperature molecular spectroscopic database, J. Quant. Spectrosc. Radiat. Transfer 111 (15) (2010) 2139–2150.

[22] L.S. Rothman, I.E. Gordon, A. Barbe, D.C. Benner, P.F. Bernath, M. Birk, V. Boudon, L.R. Brown, A. Campargue, J.P. Champion, K. Chance, L.H. Coudert, V. Dana, V.M. Devi, S. Fally, J.M. Flaud, R.R. Gamache, A. Goldman, D. Jacquemart, I. Kleiner, N. Lacome, W.J. Lafferty, J.Y. Mandin, S.T. Massie, S.N. Mikhailenko, C.E. Miller, N. Moazzen-Ahmadi, O.V. Naumenko, A.V. Nikitin, J. Orphal, V.I. Perevalov, A. Perrin, A. Predoi-Cross, C.P. Rinsland, M. Rotger, M. Simeckov, M.A.H. Smith, K. Sung, S.A. Tashkun, J. Tennyson, R.A. Toth, A.C. Vandaele, J. Vander Auwera, The HITRAN 2008 molecular spectroscopic database, J. Quant. Spectrosc. Radiat. Transfer 110 (9–10) (2009) 533–572.

[23] R.J. Barber, J. Tennyson, G.J. Harris, R.N. Tolchenov, A high-accuracy computed water line list, Mon. Not. R. Astron. Soc. 368 (3) (2006) 1087–1094.

[24] A. Soufiani, J.-P. Martin, J.-C. Rolon, L. Brenez, Sensitivity of temperature and concentration measurements in hot gases from FTIR emission spectroscopy, J. Quant. Spectrosc. Radiat. Transfer 73 (2002) 317–327.

[25] C. Delaye, J.-M. Hartmann, J. Taine, Calculated tabulations of H_2O line broadening by H_2O, N_2, O_2 and CO_2 at high temperature, Appl. Opt. 28 (1989) 5080–5087.

[26] M. Vidler, J. Tennyson, Accurate partition function and thermodynamic data for water, J. Chem. Phys. 113 (21) (2000) 9766–9771.

[27] S. Clough, F. Kneizys, R. Davies, Line shape and the water vapor continuum, Atmos. Res. 23 (1989) 229–241.

[28] D. Goorvitch, Infrared CO line list for the $X^1\Sigma^+$ state, Astrophys. J. Suppl. S. 95 (2) (1994) 535–552.

[29] Y. Babou, P. Rivière, M.Y. Perrin, A. Soufiani, High-temperature and nonequilibrium partition function and thermodynamic data of diatomic molecules, Int. J. Thermophys. 30 (2) (2009) 416–438.

[30] M.-Y. Perrin, A. Soufiani, Approximate radiative properties of methane at high temperature, J. Quant. Spectrosc. Radiat. Transfer 103 (1) (2007) 3–13.

[31] W. Malkmus, Random Lorentz band model with exponential-tailed S^{-1} line intensity distribution function, J. Opt. Soc. Am. 57 (1967) 323–329.

[32] P. Rivière, A. Soufiani, Generalized Malkmus line intensity distribution for CO_2 infrared radiation in Doppler broadening regime, J. Quant. Spectrosc. Radiat. Transfer 112 (2011) 475–485.

[33] D. Scutaru, L. Rosenmann, J. Taine, Approximate intensities of CO_2 hot bands at 2.7, 4.3, and 12 μm for high temperature and medium resolution applications, J. Quant. Spectrosc. Radiat. Transfer 52 (6) (1994) 765–781.

[34] S. Depraz, A. Perrin, M.-Y. Soufiani, Infrared emission spectroscopy of CO_2 at high temperature. Part I: Experimental setup and source characterization, J. Quant. Spectrosc. Radiat. Transfer 113 (2012) 1–13.

[35] V. Goutiere, F. Liu, A. Charette, An assessment of real-gas modelling in 2D enclosures, J. Quant. Spectrosc. Radiat. Transfer 64 (3) (2000) 299–326.